

## Article

# Investigating Thermal Controls on the Hyporheic Flux as Evaluated Using Numerical Modeling of Flume-Derived Data

Jake W. Riedel <sup>1</sup>, Eric W. Peterson <sup>1,\*</sup> , Toby J. Dogwiler <sup>2</sup>  and Wondwosen M. Seyoum <sup>1</sup> 

<sup>1</sup> Department of Geography, Geology, and the Environment, Illinois State University, 101 South School Street, Campus Box 4400, Normal, IL 61790, USA

<sup>2</sup> Department of Geography, Geology, and Planning, Missouri State University, Springfield, MO 65897, USA

\* Correspondence: ewpeter@ilstu.edu; Tel.: +1-309-438-7865

**Abstract:** The flux of water through the hyporheic zone (HZ) is controlled by stream bedforms, sinuosity, surface water velocity, local water table, seasonality, and hydraulic conductivity (K) of the bed material. Dependent on both the kinematic viscosity and density of water, K values are a function of temperature. In most studies, changes in temperature have been neglected because of the limited effect either density or viscosity has on K values. However, these variations are important given the role of K in HZ flux, which lead to the hypothesis that flow into the HZ would be more efficient (faster rate and greater depth) under warmer conditions than under cool conditions. To discern how water temperature affects flow depth in the HZ, VS2DHI simulations were created to map flow under both warm and cool thermal conditions. The models employed data collected from a series of varying temperature hydrologic flume tests in which the effects of hyporheic flow altering variables such as sinuosity, surface water velocity and volume, and bed-forms were controlled. Results verify that K values in the HZ were larger under warm conditions generating deeper HZ pathways, while the smaller K values under cool conditions produced shallower pathways. The simulations confirmed a faster speed of frontal movement under warm conditions than cool. Péclet numbers revealed a shallower advective extinction depth under cool conditions as opposed to warm.

**Keywords:** hyporheic flux; thermal transport; hydraulic conductivity; Péclet numbers



**Citation:** Riedel, J.W.; Peterson, E.W.; Dogwiler, T.J.; Seyoum, W.M. Investigating Thermal Controls on the Hyporheic Flux as Evaluated Using Numerical Modeling of Flume-Derived Data. *Hydrology* **2022**, *9*, 156. <https://doi.org/10.3390/hydrology9090156>

Academic Editor: Monzur A. Imteaz

Received: 15 July 2022

Accepted: 28 August 2022

Published: 30 August 2022

**Publisher's Note:** MDPI stays neutral with regard to jurisdictional claims in published maps and institutional affiliations.



**Copyright:** © 2022 by the authors. Licensee MDPI, Basel, Switzerland. This article is an open access article distributed under the terms and conditions of the Creative Commons Attribution (CC BY) license (<https://creativecommons.org/licenses/by/4.0/>).

## 1. Introduction

Heat is a useful tracer to study groundwater flow to, from, and throughout the subsurface. In addition to being a naturally occurring and cost-effective tracer, heat can be interpreted for tracking groundwater fluxes [1], delineating portions of gaining and losing streams [2], and studying other parameters such as hydraulic conductivity and flow [3]. Stallman brought attention to the use of subsurface temperature gradients as an indirect measurement of groundwater flow velocity and porosity from the use of partial differential equations [4]. As a tracer, heat has been employed primarily to quantify groundwater discharge and to identify areas of surface and groundwater interaction [2,3,5]. Temperature data can be utilized for complex modeling of subsurface groundwater movement, including three-dimensional velocity flow fields and alterations of flow redirected by in-stream structures [6,7]. Two- and one-dimensional models of heat flow have been made increasingly user-friendly and accessible over recent years because of the release of free modeling software such as VS2DHI, which has the power to describe subsurface energy transport with a user-friendly and efficient GUI [8].

The subsurface area directly beneath the stream hosting the mixture of upwelling groundwater and downwelling surface water is known as the hyporheic zone (HZ) [9]. Temperature tracers have become a popular tool in the study of flow in the hyporheic zone and have been proven to be a strong resource for quantifying groundwater/surface water exchanges [10–18]. The temperature gradient of the HZ is influenced by the individual temperatures of either the surface water or the groundwater [19].

Direction and magnitude of hyporheic fluxes are controlled primarily by the hydrologic conditions of the streambed and the regional water table forcing exchange via modifications to the local pressure field. Some streambed controls include hydraulic conductivity, sediment composition, channel morphology (bed-form, sinuosity), seasonality, and, ultimately, the local pressure field [20–23]. Hydraulic conductivity, a function of the streambed medium and the density and viscosity of the fluid, impacts velocity and direction of hyporheic flux and can be defined as the ease with which fluid moves through the medium. Hyporheic exchange is unlikely or minimal in streambed mediums with low hydraulic conductivity.

Previous work studying the dynamism of substrate thermal responses to storm events concludes heat propagation within stream substrate differs seasonally, suggesting that temperature influences flow dynamics in the HZ [14,19,24]. While monitoring a low gradient, gaining stream, Oware and Peterson [24] reported that during warm periods the thermal front in the HZ extended to 90 cm depth, while during cool periods in the same setting, the front only extended to 60 cm. Often, changes in viscosity and density of water from temperature changes are neglected because of the small effect viscosity and density has on hydraulic conductivity [22]. When the water temperature fluctuates between the range observed by Oware and Peterson, 0.1 °C to 30 °C, the difference in water density is at most 4 kg/m<sup>3</sup>, and the difference in viscosity is 0.989 kg/(m·s). These differences result in a theoretical difference in hydraulic conductivity less than an order of magnitude, which can be viewed as within the error measurement of hydraulic conductivity values. However, these changes are important to understand because an increase (or decrease) in hydraulic conductivity will result in a corresponding change in groundwater velocity, which has implications relating to residence time, flux rates, subsurface nutrient processing, biogeochemical activities [25–28]. With these observations in mind, the logical next step is to recreate a HZ environment where controls can be put in place to observe changes when the only variable is temperature.

We hypothesized that flow into the stream substrate would be more efficient (faster rate and greater depth) under warmer conditions and lower under cool conditions, warranting more stewardship in including the effects of temperature in modeling small-scale environments. Using a similar method as described in Bastola and Peterson [19], multiple two-dimensional inverse models were created using V2SDHI to determine flow characteristics under both warm and cool thermal conditions. Experimental data were collected from a series of flume trials where variables that affect hyporheic flux (regional gradient, bedforms, etc.) were held constant except for water temperature. The implementation of consistent conditions using a flume allowed for a detailed examination of temperature on flux, whereas high levels of scrutiny are required to analyze those specific controls on a highly variable in situ stream [20]. The experimental design provided an easy transition to modeling software that uses a modified advection–dispersion equation to model fluid flow based on changes in temperature [8]. Failing to integrate temperature variability may result in significant error in estimating hyporheic flux rates and residence times [29]. Additionally, understanding these changes could help prepare mitigation countering the effects of future urban expansion, climate change, and other changes that modify surface and groundwater temperatures.

## 2. Materials and Methods

### 2.1. Data Acquisition: Flume Trials

The development of our understanding of heat flow as a proxy to groundwater flow, coupled with improvements in modeling techniques utilizing heat as a tracer, enables us to accurately analyze ground-surface water interactions [9,30–32]. In 2009, a series of flume trials were conducted within a hydraulic channel (flume) that measured 4.5 m long × 0.32 m wide × 0.4 m deep (Figure 1). To account for the controls on hyporheic flux and isolate temperature, the flume was filled with a homogeneous (80%), well-sorted, very coarse-grained sand (from 1 to 2 mm), with the remainder being coarse (from 0.5 to

1 mm) and medium (from 0.25 to 0.5 mm) grained sand. Prior to placement in the flume, the sand was well mixed with an average porosity of 0.40. Along the flume, seven arrays of four temperature loggers (HOBO U12-012, with a resolution of 0.03 °C and accuracy of  $\pm 0.35$  °C) were installed with a longitudinal spacing of 0.5 m starting at 1.0 m from the upstream end of the channel. The loggers had a vertical spacing of 0.07 m starting from the bottom of the channel (Figure 1). The temperature was recorded every 5–15 s (some trials varied) for the duration of the trial.

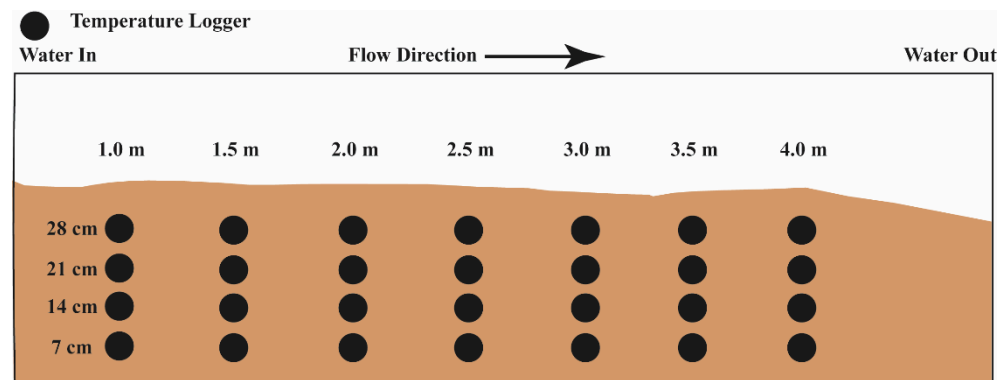


**Figure 1.** Conceptual model of hydraulic channel. The black circles represent the location of the temperature loggers. Loggers were placed uniformly within the substrate, vertically every 7 cm from the bottom of the flume, with a horizontal spacing of 0.5 m.

A total of 34 trials were conducted alternating between warm and cool surface water inputs. To simulate streams under a continental mid-latitude climate, for half of the trials, cool water and ice were added to the 950 L reservoir to lower the water temperature to 17 °C (simulating spring or fall conditions). For the other half of the trials, warm water was added to raise the initial water temperature to 27 °C (simulating summer conditions). Once the reservoir water reached the required temperature, the trial was initiated by starting flow through the channel. The only temperature changes beyond this point for each trial were caused by natural atmospheric attenuation. For each trial, slope, air temperature, and discharge (velocity) were kept constant. Slope was maintained consistently at 0.5% among all trails. The streamflow through the channel was maintained at constant discharge, either 8.5 L/s or 4.9 L/s. Trials typically lasted about 24 h, ending when the surface water temperature reached an equilibrium with room temperature, approximately 22 °C. The subsurface temperature was not required to reach equilibrium to complete the trials; however, a uniform temperature throughout the system was required before a subsequent trial was initiated. While natural streams experience temporal rearrangement of the streambed [33], sediment redistribution of the flume was not incorporated into the experimental design.

## 2.2. Numerical Modeling: VS2DHI

While the flume trials provide temporal and spatial temperature data, direction and magnitude of flow, and physical properties (e.g., hydraulic conductivity), were not obtained from the trials. A transient, 2-D, homogeneous model was set up to simulate the system in VS2DHI [8], a public-domain thermal modeling software from the USGS. Model domain was ascertained from laser line measurements provided before each flume trial. Initial model conditions included temperature, initial equilibrium profile, head at each modeled boundary condition, and thermal and other physical transport properties of both the medium and fluid (Table 1). The time-step varied from 5 to 15 s depending on the resolution of the temperature loggers. Boundary conditions were set as follows: left, right, and bottom sides as no-flow ( $\frac{\partial h}{\partial x} = 0$ ), no-flux boundaries ( $\frac{\partial T}{\partial x} = 0$ ), and the top of the domain was split into nine (9) equal-length specified head and specified temperature boundaries. For the recharge periods, the specified head values were held constant, but the temperatures

varied based on the temperature of the surface water. In VS2DHI, recharge periods are considered timeframes of equal temperature.

**Table 1.** Initial physical model parameters.

Flume Trial	Surface Slope (%)	Pump Rate (L/s)	Air Temperature (°C)	Water Temperature (°C)
Cool 1	0.5	8.5	21.5	16.1
Cool 2	0.5	8.5	22.3	13.6
Cool 3	0.5	4.9	22.3	15.6
Warm 1	0.5	8.5	22.0	29.9
Warm 2	0.5	8.5	22.4	30.1
Warm 3	0.5	4.9	21.9	30.5

Observation points were added to the model at the same location temperature probes were installed in the flume to provide output data for the calibration process. Model simulations were run to analyze differences in flow with different thermal conditions solved via the advection–dispersion equation (Equation (1)):

$$\frac{\partial}{\partial t}[\theta C_w + (1 - n)C_s]T = \nabla \cdot K_t(\theta)\nabla T + \nabla \cdot \theta C_w D_h \nabla T - \nabla \cdot \theta C_w q T + j C_w T^\circ \quad (1)$$

where  $\theta$  represents volumetric moisture content,  $C_w$  is heat capacity of water,  $C_s$  is heat capacity of dry solid,  $n$  is porosity,  $T$  is temperature in °C,  $K_t$  is the thermal conductivity of the water and solid matrix,  $D_h$  is the coefficient of hydrodynamic dispersion,  $q$  is the specific discharge,  $j$  is the rate of the source fluid, and  $T^\circ$  is the temperature of the source fluid in °C [8]. The  $q$  is a function of head and hydraulic conductivity ( $K$ ) and the hydraulic gradient ( $i$ ),  $q = Ki$ . Initial values for the parameters are provided in Table 2. VS2DHI simultaneously calculates  $T$  and  $q$  based on the infiltrating temperature plume delineated by assigned boundary conditions. In addition to the models based on flume data, an additional theoretical cold temperature model was created utilizing the same domain. This was to allow for a larger range of model temperatures to include in our interpretation.

**Table 2.** Initial model parameter values.

Parameter	Value Range
Hydraulic conductivity ( $\text{m s}^{-1}$ )	$9 \times 10^{-7}$ – $6 \times 10^{-3}$ <sup>a</sup>
Heat capacity ( $\text{J m}^{-3} \text{K}^{-1}$ )	
Solid	$1.1 \times 10^6$ – $1.3 \times 10^6$ <sup>b</sup>
Liquid	$4.2 \times 10^6$ <sup>b</sup>
Saturated solid	$2.5 \times 10^6$ – $3.2 \times 10^6$ <sup>b</sup>
Porosity	0.30–0.50 <sup>c</sup>
Thermal conductivity ( $\text{W m}^{-1} \text{K}^{-1}$ )	1.4–2.2 <sup>b</sup>
Dispersivity	0.0005 <sup>b</sup>

<sup>a</sup> Values sourced from [34]. <sup>b</sup> Values sourced from [19]. <sup>c</sup> Values sourced from [35].

### 2.3. VS2DHI Calibration

Model calibration is a fine-tuning process that involves making small modifications to model parameters until the model best represents the observed data. Since VS2DHI does not have a calibration function, R programming was employed to streamline the process. Calibration was based on the reduction of the error between the measured temperature to the simulated temperature. The goal was to reach a root mean square error (RMSE) of 0.7 °C. Hydraulic conductivity, heat capacity of the solid and liquid, dispersivity, and saturated thermal conductivity were all used in tuning the model. In the end, hydraulic

conductivity was the most sensitive parameter, and calibration was based primarily off that value.

#### 2.4. Data Processing

Expected hydraulic conductivity (K) was calculated based on water temperature throughout each trial using the following equation (Equation (2)):

$$K = \frac{k\rho g}{\mu} \quad (2)$$

where  $k$  is the permeability of the medium,  $r$  is fluid density,  $g$  is gravitational acceleration, and  $\mu$  is fluid viscosity. Fluid density and viscosity are temperature-dependent variables and are expected to change throughout time. The expected K value was then compared to the calibrated K value and other trials to analyze in what direction it deviates under warm or cool conditions.

Using the flume data as input, VS2DHI interpolates heat flux using a finite-difference model and returns the resultant specific discharge ( $q$ ) throughout the model. The  $q$  value was used along with the model parameters mentioned above to solve for the Péclet number (Pe) at each node in the model. The Pe represents the ratio of advective to conductive transport and provides insight into the movement of fluid in a system. Advection can be described as the transference of heat via the physical movement of water, and conduction can be described as the transference of heat via molecular spreading. The ratio is calculated as follows (Equation (3)):

$$Pe = \frac{q\Delta z\rho C}{2K_t} \quad (3)$$

where  $q$  is the specific discharge at a cell in the model,  $\Delta z$  is the representative depth (the depth from the surface),  $\rho$  is fluid density,  $C$  is fluid-specific heat, and  $K_t$  is thermal conductivity [36]. The average  $q$  value each depth in the model domain was also compared between all trials to see its deviation with temperature and depth.

### 3. Results

Results of the six computed models are reported in Table 3. Only three models of each temperature were created as they provided consistent results, and more models would not provide much more utility in answering our research questions. The RMSEs (0.33–0.65 °C) for these models are reasonable as surface temperature changes are rapid and sheer upon slug input. Each model has an associated heat-map overlain with  $q$  values and average Pe numbers. An additional theoretical cold trial was simulated to represent a temperature of 5 °C to analyze conditions representative of cold season stream temperatures, as experimental runs only highlighted slight changes in temperature.

**Table 3.** Model results of cool runs 1–3, warm runs 1–3, and the theoretical cold run (a).

Trial	Ex. Depth (cm)	Specific Discharge (m/s)	Avg. T (HZ) (°C)	RMSE (°C)	Modeled K (m/s)	Calculated K (m/s)
Cool 1	21	$2.1 \times 10^{-5}$	20.5	0.55	0.0009	0.0010
Cool 2	21	$2.8 \times 10^{-5}$	20.9	0.62	0.0018	0.0009
Cool 3	21	$2.1 \times 10^{-5}$	20.8	0.57	0.0018	0.0010
Warm 1	26	$4.3 \times 10^{-5}$	23.8	0.65	0.0022	0.0011
Warm 2	26	$3.5 \times 10^{-5}$	23.3	0.33	0.0020	0.0011
Warm 3	25	$3.1 \times 10^{-5}$	22.9	0.59	0.0020	0.0011
Cold a	13	$9.3 \times 10^{-6}$	8	-	0.0001	0.0007

The calculated  $q$  values of these models help describe how the speed of water varies under different thermal conditions (Figure 2). The range of  $q$  for cold trials was  $1.3 \times 10^{-5}$  to  $4.3 \times 10^{-5}$  m/s, mostly less than the range of flux for warm trials,  $2.2 \times 10^{-5}$  to  $7.6 \times 10^{-5}$  m/s. Overlap was expected as the temperature ranges were similar, and some similarities between the maximum  $q$  of cold trials and the minimum  $q$  of warm trials occurred. Our theoretical cold trial highlighted how dramatic lowering of the  $q$ ; with the theoretical 5 °C trial, a  $q$  of  $9.3 \times 10^{-6}$  m/s was simulated, nearly four times less than the average warm flux (Table 3).

The design of the flume experiment initiated advective transport, which would become more prominent with increasing velocity and conduction being more significant with decreasing velocity. The advective thermal extinction depth is representative of the maximum depth of physical movement of the input water within the flume. Maps of calculated Pe numbers within the model domain revealed a distinct depth of advective extinction for each trial (Figure 3). For this analysis, the depth of extinction was treated as the depth where the average Pe number reached 2. Despite a Pe number of 1 being the logical extinction depth, a Pe number of 2 was used as some of the models did not have a depth in which 1 was reached, and a value of 2 represents a definitive advective signal. In cool runs, the average extinction depth was 21 cm, and the system lost advective signals between hyporheic flux sites where there was little interfacing between reservoirs (Figure 3a–c). The average extinction depth in warm trials was 25.6 cm (Figure 3d,e). The cold theoretical trial's extinction depth was interpreted as 13 cm, establishing a trend of decreasing extinction depths as input water temperature decreases (Figure 4f).

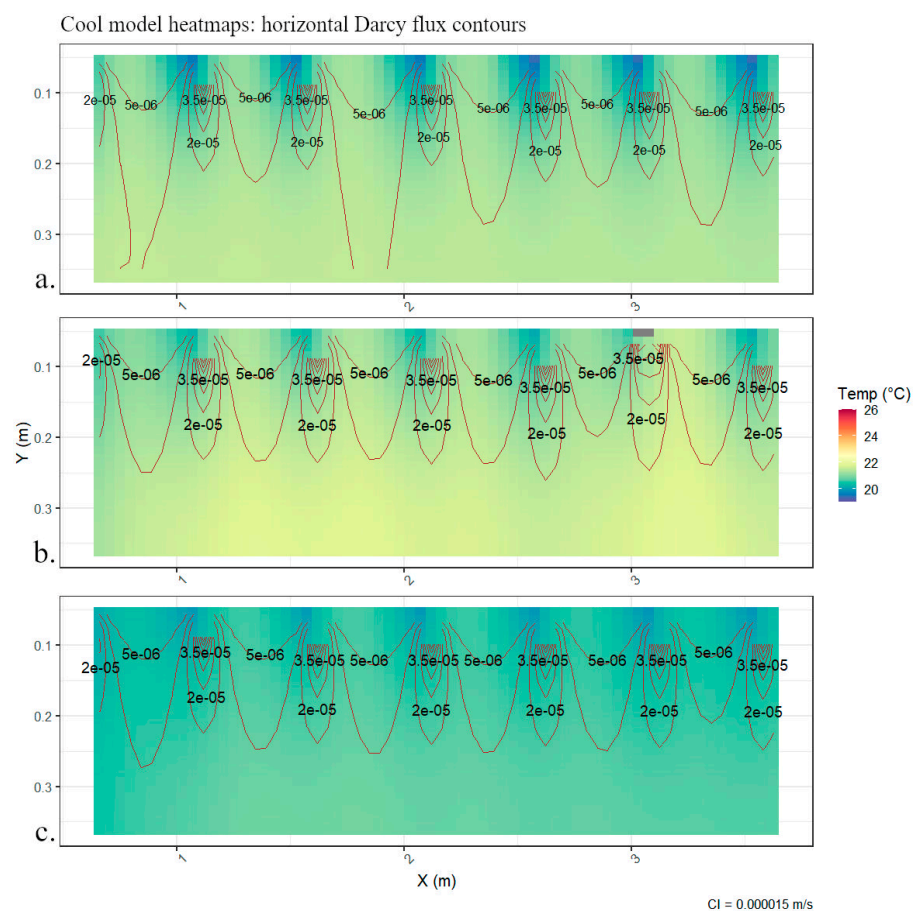
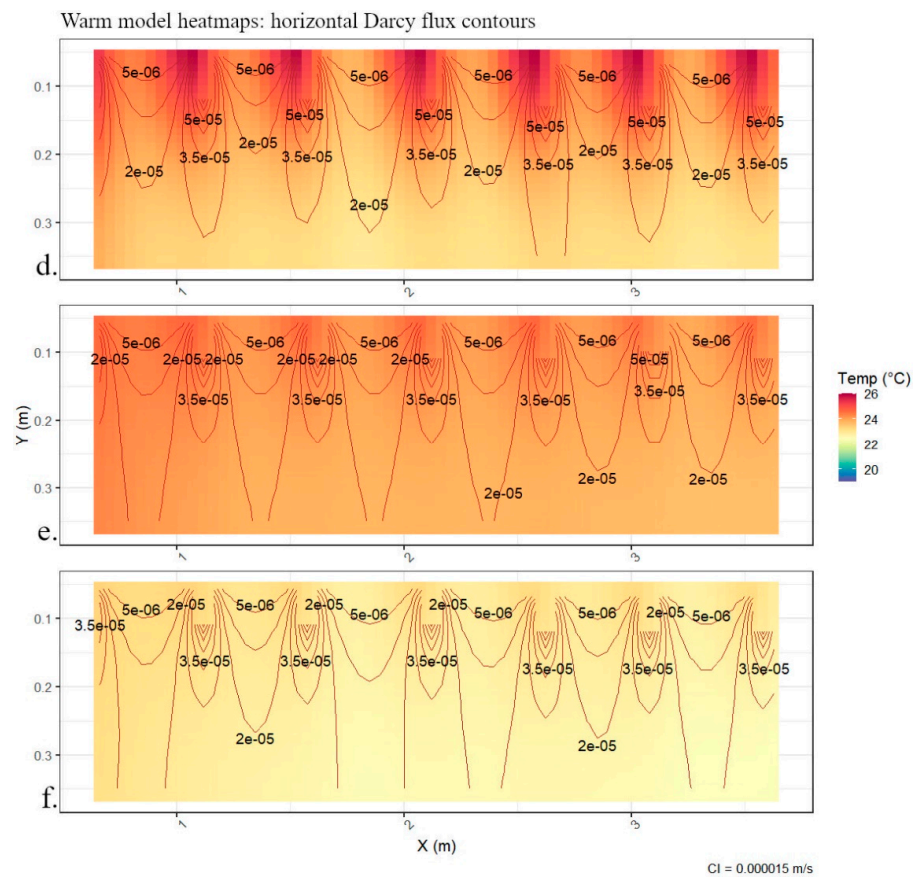
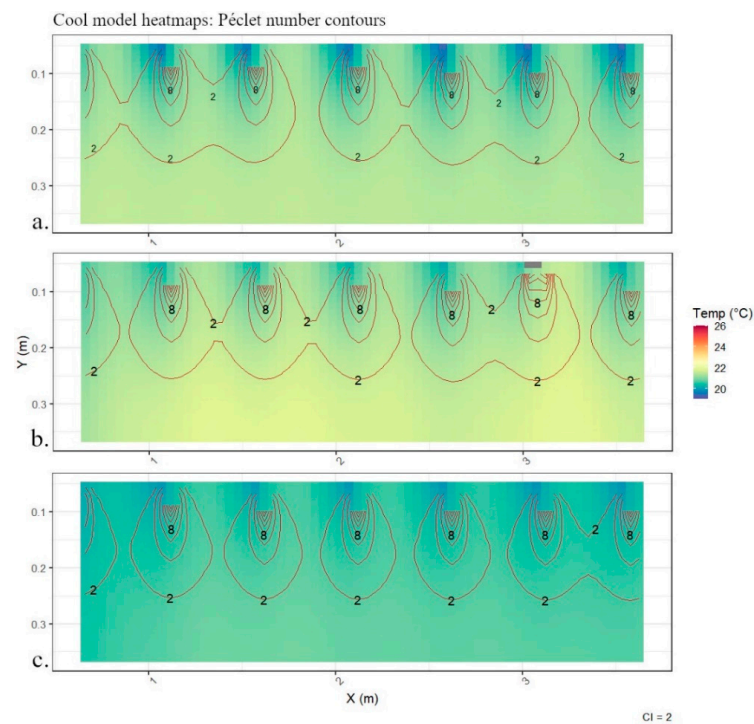


Figure 2. Cont.



**Figure 2.** Temperature heat maps of cold runs (a–c) and hot runs (d–f) overlain with contours of horizontal Darcy flux with a contour interval of 0.000015 m/s. Notice areas of highest horizontal flux are associated with temperature signatures of downwelling zones. Additionally, the shape of the contours is driven by the modeling software’s ‘step-down’ type gradient, and the actual contours would be more laterally continuous (see Section 4.1).



**Figure 3.** Cont.

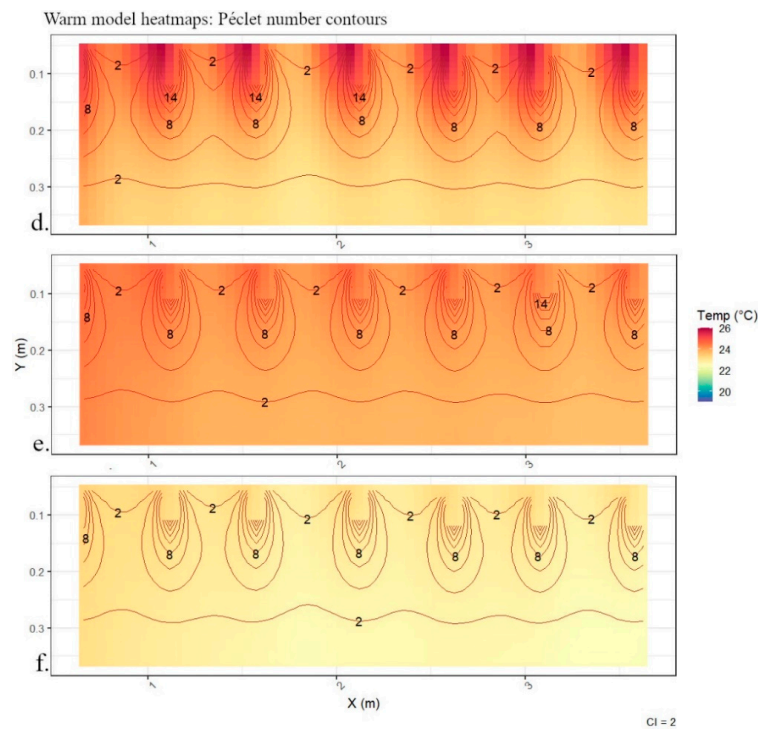


**Figure 3.** Temperature heat maps of cold runs (a–c) and hot runs (d–f) overlain with contours of Pe numbers with a contour interval of 2. Notice areas of highest Pe number are associated with temperature signatures of downwelling zones. Additionally, the shape of the contours is driven by the modeling software’s ‘step-down’ type gradient, and the actual contours would be more laterally continuous (see: Section 4.1).

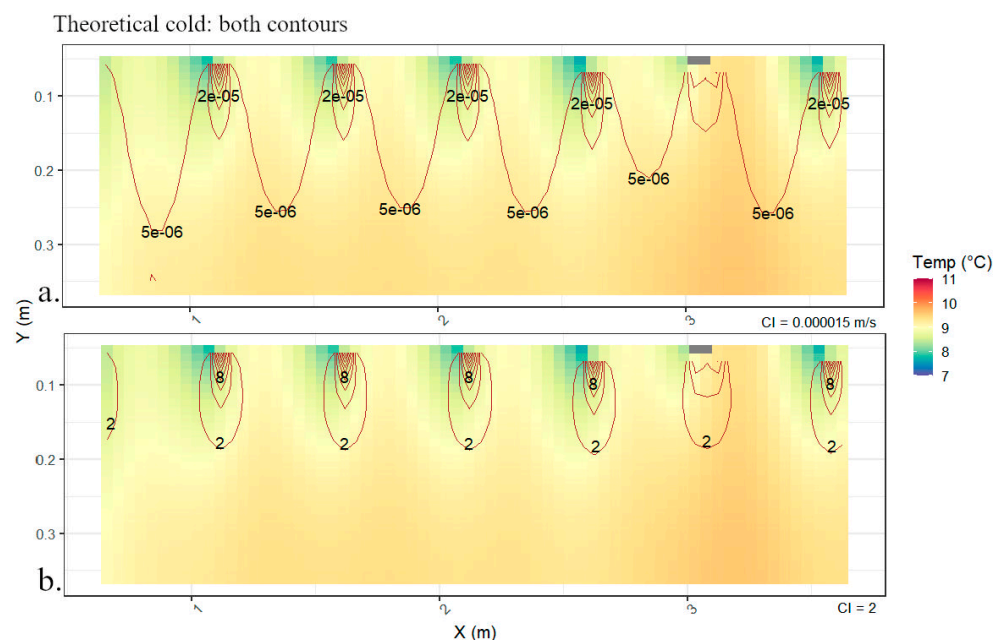


**Figure 4.** Temperature heatmaps of the theoretical cold trial with a starting ambient temperature of 10 degrees Celsius and input temperature of 5 degrees Celsius ran for 60,000 s. (a) is overlain with contours of horizontal Darcy flux (CI = 0.000015 m/s). (b) is overlain with contours of Pe number (CI = 2). Additionally, the shape of the contours is driven by the modeling software’s ‘step-down’ type gradient, and the actual contours would be more laterally continuous (see Section 4.1).

Comparing  $q$  and Pe ratios with their associated thermal regimes for each trial confirmed the expected relationship between temperature and velocity (an increase under

warm conditions, a decrease under cool conditions) and tied in predictable changes in extinction depth associated with temperature (an increase under warm conditions, a decrease under cool conditions). Flow can be interpreted as being parallel to specific discharge contours and concentrated in areas of higher Pe number. While warm and cool trials generated similar flow paths, the depth and speed at which bulk flow propagates were greater under warm conditions than cool. It is also interesting to note the significant range of Pe numbers found near-surface in warm trials, indicating more flux between surface and ground reservoirs under these conditions. Comparing the  $q$  values between the maximum warm and minimum theoretical cold trials, the warm trials had  $q$  values an order magnitude higher. Collectively, the flux and Pe ratios imply that warmer temperatures allow for enhanced subsurface flow due to advection. The influence of advection is a result of reduced viscosity of the warmer waters decreasing flow resistance and allowing for quicker flow.

#### 4. Discussion

##### 4.1. The Nature of the Model

When interpreting these results, it is critical to keep in mind the flow effects introduced by VS2DHI's limitations. VS2DHI does not allow for a traditional steady head gradient; instead, each boundary condition of the model is assigned a head, and the abrupt (albeit small) change in pressure head between boundaries drives downwelling in the system. In the actual flume, downwelling is likely forced along the upward-sloping bedform on the far left and upwelling along the downward-sloping bedform on the far right (Figure 1). It is important to note the shape of the contours overlaying our heatmaps represents this aspect, and the contours realistically should be more laterally continuous. Despite these discontinuities, understanding what is controlling flux zones and the differences between our flume and the model gives a better understanding of the hydrologic modifications of temperature in this system. Since the primary driver of SWI (surface water interface) exchange is differences in pressure, we understand why this discrepancy arises, and our gap in understanding may be reduced [22]. Additionally, the model assumes its results hold consistent with a more regular groundwater temperature.

##### 4.2. Comparisons and Applications

Comparing our results to Cardenas and Wilson [37] confirms the hydrologic changes associated with thermal setting. Cardenas and Wilson studied the influence of bedforms using temperature as a tracer, those of which behave similarly to flux between our step-down type gradients. The study, however, failed to assess alone the impacts of temperature. Their results agree that fluid flux is proportional to water temperature with strong temperature variation in downwelling zones and a return to ambient temperature in upwelling zones. Cardenas and Wilson highlighted the importance of sediment permeability, where the temperature has little effect in low permeability mediums. This makes sense as, in these settings, SWI exchange will be limited, and the water that does exchange will primarily transfer heat via conduction and the slow rate of flux.

The effects of heat on flow were also consistent with observations made by Oware and Peterson [24], which studied variations in a stream's thermal response to storms during cold and warm periods. For warm periods, they observed thermal responses to storm events at greater depths than for storms during cold periods and suggested greater advective control during warm periods. The differences in dampening of thermal amplitudes with depth under either condition are consistent with our results and help explain the rates of forcing observed within their study site. Similarly, Beach and Peterson [38] examined diel and seasonal hyporheic thermal profiles in mid-latitude streams, where groundwater temperatures were warmer than surface waters in fall and cooler than surface waters in summer. They observed hyporheic temperatures more like groundwater during fall and more like surface water during summer, indicating more influence of the groundwater component during fall. The greater thermal influence of groundwater in cold conditions

suggests a shallower depth of stream water flux than during warm conditions. Beach and Peterson [38] concluded, “The transmission of diel signals is limited by the efficiency of advection . . .”, coinciding with our results and confirming the thermal impact.

Our results can be used to modify additional hyporheic controls, for example, changes in flux under gaining and losing conditions with the addition of temperature perturbations. This can be best explained by defining “hydrologic/thermal forcing” to make separations between stream–aquifer and stream–aquifer–HZ relationships. For this section, gaining and losing will refer to aquifer-to-stream relationships, and forcing will refer to stream–aquifer–HZ relationships. Forcing can be considered as directional flow influenced by either upwelling groundwater or downwelling surface water. To clarify, gaining and losing can be considered an adjective, and forcing can be considered as a verb. Singh et al. [22] related forcing with storm events and observed an increase in forcing depth during peak flow conditions, similar to [24]. The results from these studies coupled with our results suppose that hot water resists upward forcing and supports downward forcing, and vice versa. With an already small HZ under gaining conditions and a larger HZ under losing conditions, temperature will modify this size with its relationship to forcing [20]. Since hot water supports downward forcing, the surface component of a gaining stream under hot conditions may have a slightly larger HZ than expected, while a gaining stream under cold conditions may have a much smaller HZ than expected (Figure 5). In a losing stream under cold conditions, the HZ may be slightly smaller, while under hot conditions, the HZ may be much larger (Figure 5). The differentiation in the degrees of change is a result of cool water reducing ease of flow and hot water increasing it.

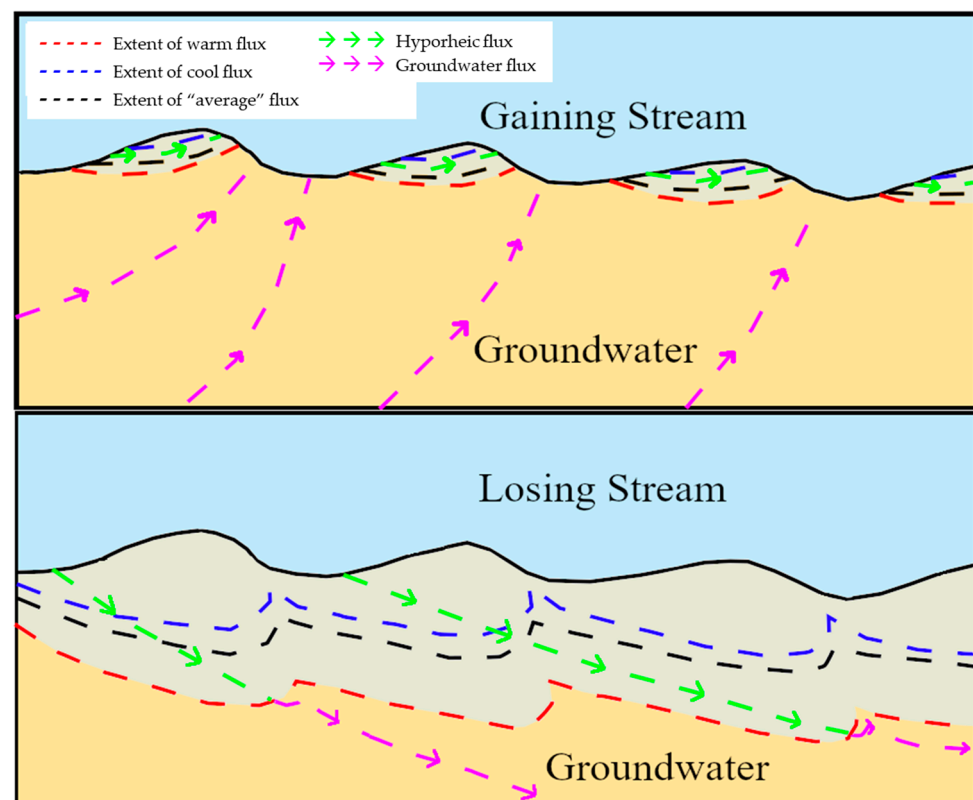


**Figure 5.** Conceptual model of alterations to HZ from temperature under gaining and losing conditions. The blue dashed line represents the theoretical extent of cool flux under either condition, and the red dashed line represents the theoretical extent of warm flux under either condition.

Under cool conditions, it may be expected that the cool surface water would move at a slower rate than the warmer groundwater; however, the concept of forcing helps explain this. With downwelling, water is forced through pores from differences in the

pressure field. This pressure difference plays a greater role in the movement of water than temperature, outweighing differences in flow rates solely caused by temperature. Remember, the temperature is not a primary driver, as other controls such as regional water table, which determines if a stream is gaining or losing, greatly outweigh it, but still has an impact and may be an accessory to other controls associated with SWI exchanges by altering the fluid's density and viscosity.

#### 4.3. Implications for Seasonal and Diel Fluctuations

Temporality is an essential aspect to consider while studying natural systems. While the surface water response is attenuated to atmospheric changes in temperature, the attenuation does not make subsurface temperature fluctuations by any means insignificant. Additionally, a continually decreasing diel amplitude of water temperature is observed with depth in the subsurface. However, this decrease is not constant and changes both seasonally and throughout the day in the top couple of meters of the subsurface. This variability may be due to changes in surface water temperature, which according to our results, water has a reduced ability to infiltrate during cool conditions and an improved ability to infiltrate during warm conditions. The thermal gradient during cool periods (winter) may have a large slope, suggesting a rapid change in thermal amplitude with depth, and the thermal gradient during warm periods (summer) may have a more gradual change, suggesting a smaller change in thermal amplitude over the same depth. Observed changes in thermal amplitudes with depth are, in part, due to changes in flow patterns associated with surface water temperatures.

Harris and Peterson [16] assessed stage as a potential control of vertical hyporheic exchange. Like [24], their raw data exhibit a deeper thermal response to storm events during winter than summer. Despite Harris and Peterson's conclusion that summer exhibits a shallower hyporheic zone than during winter, storm responses in their data relay the opposite, where the downwelling associated with peak flow events extends to a greater depth during warm periods than cool periods, highlighting the influence of surface water temperature. The discrepancy between baseline summer and winter flux (comparing [16] to this project) is due to changes in regional groundwater gradient, which outweighs the controls of temperature on hyporheic flow depth and is a clear limitation of utilizing a flume.

#### 4.4. Limitations

It would be beneficial to retest this with more robust modeling software. VS2DHI determines head at boundary conditions and thus cannot be made into a smooth gradient but more of a "step-down" gradient. This induced downwelling at these "step-down" areas and, despite calibrating well, was not a perfect representation of the flume. The flume itself initialized at room temperature and did not represent groundwater conditions, so a full hyporheic thermal gradient could not be established. It would be helpful to return to this using a deeper flume to completely capture the extent of downwelling or finding a representative in situ location. The model also does not account for movement perpendicular to flow, but in a real stream, this may only be significant nearest stream banks, and our model may serve as a good representative for conditions below the thalweg. Additionally, applying the temperature concept to other controls of SWI exchange, such as stream slope or regional groundwater table, may help in creating a fuller understanding of the association of temperature with hyporheic flux.

Direct comparison to in situ studies is limited by the design of the flume study. The flume system had no groundwater flow prior to the start of the test or during the trial. Hence, the flume did not account for groundwater upwelling or downwelling that would be expected in natural streams [23,38]. It is important to note that different groundwater signatures affect the subsurface viscosity and pressure field, resulting in different flow depths and attenuating the effects of thermal forcing.

## 5. Conclusions

Analyzing data from an experimental flume trial, which mitigated the effect of common in situ flow drivers, proved effective in identifying the influence of the thermal regime on hyporheic flow dynamics. While some authors have addressed this question, none, to our knowledge, have utilized an experimental system or addressed solely the influence of temperature [29,37]. Based on our results, we were able to interpret the following:

1. Warmer waters have decreased kinematic viscosity, thus improving the efficiency of flow in both horizontal and vertical directions. A deeper hyporheic zone along with greater and more spatially spread advective flux was observed when temperature was increased in the flume.
2. Colder waters have higher kinematic viscosity, thus reducing the efficiency of flow in both horizontal and vertical directions. A shallower hyporheic zone along with reduced and less especially spread advective flux was observed when the temperature was decreased in the flume.
3. The depth of advective thermal transport is greater in warm runs than in cold runs.
4. A significant difference in flow exists between our warmest trial and the theoretical cold run (the temperature difference of which represents a typical yearly max and min), implying a definitive impact of thermal conditions on hyporheic forcing.

These interpretations were then applied to other theoretical models of hyporheic controls such as the regional groundwater table and second were able to be observed within seasonal in situ datasets to confirm our results [16,24,38]. Additionally, thermal influence needs to be further analyzed while coupled with other flux drivers to determine how they interact. An exact quantification of residence time would also be beneficial to understanding more potential flow changes to examine if the deeper flow is extending residence time as flow velocity increases simultaneously.

**Author Contributions:** Conceptualization, J.W.R. and E.W.P.; methodology, J.W.R., T.J.D. and E.W.P.; software, J.W.R. and E.W.P.; formal analysis, J.W.R. and E.W.P.; resources, J.W.R., T.J.D. and E.W.P.; data curation, T.J.D. and E.W.P.; writing—original draft preparation, J.W.R.; writing—review and editing, J.W.R., E.W.P., W.M.S. and T.J.D.; visualization, J.W.R., E.W.P., W.M.S. and T.J.D.; supervision, E.W.P. All authors have read and agreed to the published version of the manuscript.

**Funding:** This research received no external funding.

**Institutional Review Board Statement:** Not applicable.

**Informed Consent Statement:** Not applicable.

**Data Availability Statement:** The flume data are available upon request.

**Acknowledgments:** The authors thank the Department of Geosciences at Winona State University for access to flume.

**Conflicts of Interest:** The authors declare no conflict of interest.

## References

1. Silliman, S.E.; Ramirez, J.; McCabe, R.L. Quantifying downflow through creek sediments using temperature time series: One-dimensional solution incorporating measured surface temperature. *J. Hydrol.* **1995**, *167*, 99–119. [[CrossRef](#)]
2. Silliman, S.E.; Booth, D.F. Analysis of time-series measurements of sediment temperature for identification of gaining vs. losing portions of Juday Creek, Indiana. *J. Hydrol.* **1993**, *146*, 131–148. [[CrossRef](#)]
3. Lapham, W.W. Use of temperature profiles beneath streams to determine rates of vertical ground-water flow and vertical hydraulic conductivity. *Water-Supply Pap.* **1989**, *2337*, 35.
4. Stallman, R.W. Computation of ground-water velocity from temperature data. *USGS Water Supply Pap.* **1963**, *1544*, 36–46.
5. Briggs, M.A.; Lautz, L.K.; Buckley, S.F.; Lane, J.W. Practical limitations on the use of diurnal temperature signals to quantify groundwater upwelling. *J. Hydrol.* **2014**, *519*, 1739–1751. [[CrossRef](#)]
6. Zlotnik, V.; Tartakovsky, D.M. Interpretation of heat-pulse tracer tests for characterization of three-dimensional velocity fields in hyporheic zone. *Water Resour. Res.* **2018**, *54*, 4028–4039. [[CrossRef](#)]
7. Menichino, G.T.; Hester, E.T. Hydraulic and thermal effects of in-stream structure-induced hyporheic exchange across a range of hydraulic conductivities. *Water Resour. Res.* **2014**, *50*, 4643–4661. [[CrossRef](#)]

8. Healy, R.W.; Ronan, A.D. *Documentation of Computer Program VS2DH for Simulation of Energy Transport in Variably Saturated Porous Media: Modification of the U.S. Geological Survey's Computer Program VS2DT*; United States Geological Survey: Denver, CO, USA, 1996; p. 36.
9. Conant, B., Jr. Delineating and quantifying ground water discharge zones using streambed temperatures. *Ground Water* **2004**, *42*, 243–257. [[CrossRef](#)]
10. Keery, J.; Binley, A.; Crook, N.; Smith, J.W.N. Temporal and spatial variability of groundwater–surface water fluxes: Development and application of an analytical method using temperature time series. *J. Hydrol.* **2007**, *336*, 1–16. [[CrossRef](#)]
11. Hatch, C.E.; Fisher, A.T.; Revenaugh, J.S.; Constantz, J.; Ruehl, C. Quantifying surface water–groundwater interactions using time series analysis of streambed thermal records: Method development. *Water Resour. Res.* **2006**, *42*, 1–14. [[CrossRef](#)]
12. Luce, C.H.; Tonina, D.; Gariglio, F.; Applebee, R. Solutions for the diurnally forced advection–diffusion equation to estimate bulk fluid velocity and diffusivity in streambeds from temperature time series. *Water Resour. Res.* **2013**, *49*, 488–506. [[CrossRef](#)]
13. Constantz, J.; Cox, M.H.; Su, G.W. Comparison of heat and bromide as ground water tracers near streams. *Ground Water* **2003**, *41*, 647–656. [[CrossRef](#)] [[PubMed](#)]
14. Hatch, C.E.; Fisher, A.T.; Ruehl, C.R.; Stemler, G. Spatial and temporal variations in streambed hydraulic conductivity quantified with time-series thermal methods. *J. Hydrol.* **2010**, *389*, 276–288. [[CrossRef](#)]
15. Irvine, D.J.; Briggs, M.A.; Lautz, L.K.; Gordon, R.P.; McKenzie, J.M.; Cartwright, I. Using Diurnal Temperature Signals to Infer Vertical Groundwater–Surface Water Exchange. *Groundwater* **2017**, *55*, 10–16. [[CrossRef](#)] [[PubMed](#)]
16. Harris, F.C.; Peterson, E.W. 1-D Vertical Flux Dynamics in a Low-Gradient Stream: An Assessment of Stage as a Control of Vertical Hyporheic Exchange. *Water* **2020**, *12*, 16. [[CrossRef](#)]
17. Rau, G.C.; Andersen, M.S.; McCallum, A.M.; Roshan, H.; Acworth, R.I. Heat as a tracer to quantify water flow in near-surface sediments. *Earth-Sci. Rev.* **2014**, *129*, 40–58. [[CrossRef](#)]
18. McCallum, A.M.; Andersen, M.S.; Rau, G.C.; Acworth, R.I. A 1-D analytical method for estimating surface water–groundwater interactions and effective thermal diffusivity using temperature time series. *Water Resour. Res.* **2012**, *48*, 2815–2829. [[CrossRef](#)]
19. Bastola, H.; Peterson, E.W. Heat tracing to examine seasonal groundwater flow beneath a low-gradient stream. *Hydrogeol. J.* **2016**, *24*, 181–194. [[CrossRef](#)]
20. Cardenas, M.B. Stream–aquifer interactions and hyporheic exchange in gaining and losing sinuous streams. *Water Resour. Res.* **2009**, *45*, 1–13. [[CrossRef](#)]
21. Fox, A.; Boano, F.; Arnon, S. Impact of losing and gaining streamflow conditions on hyporheic exchange fluxes induced by dune-shaped bed forms. *Water Resour. Res.* **2014**, *50*, 1895–1907. [[CrossRef](#)]
22. Singh, T.; Wu, L.; Gomez-Velez, J.D.; Lewandowski, J.; Hannah, D.M.; Krause, S. Dynamic hyporheic zones: Exploring the role of peak flow events on bedform-induced hyporheic exchange. *Water Resour. Res.* **2019**, *55*, 218–235. [[CrossRef](#)]
23. Peterson, E.W.; Hayden, K.M. Transport and Fate of Nitrate in the Streambed of a Low-Gradient Stream. *Hydrology* **2018**, *5*, 55. [[CrossRef](#)]
24. Oware, E.K.; Peterson, E.W. Storm Driven Seasonal Variation in the Thermal Response of the Streambed Water of a Low-Gradient Stream. *Water* **2020**, *12*, 2498. [[CrossRef](#)]
25. Webb, B.W.; Hannah, D.M.; Moore, R.D.; Brown, L.E.; Nobilis, F. Recent advances in stream and river temperature research. *Hydrol. Process. Int. J.* **2008**, *22*, 902–918. [[CrossRef](#)]
26. Lee, R.M.; Rinne, J.N. Critical thermal maxima of five trout species in the southwestern United States. *Trans. Am. Fish. Soc.* **1980**, *109*, 632–635. [[CrossRef](#)]
27. Hester, E.T.; Doyle, M.W. Human Impacts to River Temperature and Their Effects on Biological Processes: A Quantitative Synthesis. *JAWRA J. Am. Water Resour. Assoc.* **2011**, *47*, 571–587. [[CrossRef](#)]
28. Hanaki, K.; Wantawin, C.; Ohgaki, S. Nitrification at low levels of dissolved oxygen with and without organic loading in a suspended-growth reactor. *Water Res.* **1990**, *24*, 297–302. [[CrossRef](#)]
29. Wu, L.; Singh, T.; Gomez-Velez, J.; Nützmann, G.; Wörman, A.; Krause, S.; Lewandowski, J. Impact of dynamically changing discharge on hyporheic exchange processes under gaining and losing groundwater conditions. *Water Resour. Res.* **2018**, *54*, 10076–10093. [[CrossRef](#)]
30. Anderson, M.P. Heat as a ground water tracer. *Ground Water* **2005**, *43*, 951–968. [[CrossRef](#)]
31. Constantz, J. Heat as a tracer to determine streambed water exchanges. *Water Resour. Res.* **2008**, *44*, 1–20. [[CrossRef](#)]
32. Constantz, J. Interaction between stream temperature, streamflow, and groundwater exchanges in alpine streams. *Water Resour. Res.* **1998**, *34*, 1609–1615. [[CrossRef](#)]
33. Peterson, E.W.; Sickbert, T.B.; Moore, S.L. High frequency stream bed mobility of a low-gradient agricultural stream with implications on the hyporheic zone. *Hydrol. Process.* **2008**, *22*, 4239–4248. [[CrossRef](#)]
34. Domenico, P.A.; Schwartz, F.W. *Physical and Chemical Hydrogeology*; John Wiley & Sons: New York, NY, USA, 1990; p. 824.
35. Earle, S. *Physical Geology*; BCcampus: Victoria, BC, Canada, 2015.
36. Deming, D. *Introduction to Hydrogeology*; McGraw-Hill College: New York, NY, USA, 2002; p. 468.
37. Cardenas, M.B.; Wilson, J.L. Thermal regime of dune-covered sediments under gaining and losing conditions. *J. Geophys. Res.* **2007**, *112*, 1–12. [[CrossRef](#)]
38. Beach, V.; Peterson, E.W. Variation of hyporheic temperature profiles in a low gradient third-order agricultural stream—A statistical approach. *Open J. Mod. Hydrol.* **2013**, *3*, 55–66. [[CrossRef](#)]